Eur. Phys. J. C (2020) 80:576
https://doi.org/10.1140/epjc/s10052-020-8162-9

THE EUROPEAN PHYSICAL JOURNAL C

Regular Article - Theoretical Physics

A ϕ^6 soliton with a long-range tail

André Amado[a], **Azadeh Mohammadi**[b]

Departamento de Física, Universidade Federal de Pernambuco, Recife, Pernambuco 52171-900, Brazil

Received: 14 April 2020 / Accepted: 15 June 2020 / Published online: 27 June 2020

Abstract We propose an analytically solvable sextic potential model with non-trivial soliton solutions connecting the trivial vacua. The model does not respect parity symmetry, and like ϕ^4 theory has two minima. The soliton solutions and the consequent results are obtained in terms of the Lambert W function, i.e., the inverse function of $f(W) = We^W$. They have power-law asymptotics at one spatial infinity and exponential asymptotics at the other. We compare the solution with the kink of ϕ^4 theory, which preserves the parity symmetry and has exponential asymptotics at both spatial infinities. Moreover, we study the full spectrum (bound and continuum states) of boson and fermion fields in the presence of the proposed soliton. We consider two types of coupling for the boson–soliton interaction and Yukawa coupling for the fermion–soliton interaction. Most results are derived analytically. This property renders the model a fertile ground for further study, including parity breaking related phenomena and long-range soliton–soliton interactions.

1 Introduction

There is a small class of nonlinear differential equations with soliton solutions. A soliton is a stable solution with localized energy density. It arises as a consequence of the interaction between nonlinearity and dispersion when a nonlinear sharpening term counterbalances the dispersive term. The competition between these two contributions shapes the structure of the soliton and provides its stability. In the language of topology, the soliton configuration has an associated conserved topological charge or winding number, which protects it against decay into a trivial configuration. Solitons are fascinating due to their mathematical properties. However, their usefulness extends far beyond that, touching multiple areas of science. In particular, they are subject of research in diverse areas of physics, including high energy physics, nonlinear optics and condensed matter physics [1–5]. Amongst the most known solitons are skyrmions and domain walls in magnetic materials [6–8], vortices in superconductors and fluids [9–12] as well as magnetic monopoles, Q-balls, cosmic strings and instantons in high-energy physics [13–21]. Besides the theoretical applications of solitons, they play an increasingly important role in technology, e.g., in communications [22–24].

Since the solitons are not isolated objects in most physical systems, their interaction with other fields has been subject to intense research in the literature. Boson and Dirac fields interacting with a soliton are known to affect or even create many intriguing phenomena including vacuum polarization and Casimir effect [25,26], superconductivity and Bose–Einstein condensation [27,28], localization of fermions in the braneworld scenarios [29], charge and fermion number fractionalization [30] as well as conducting polymers [31]. Massless Dirac fermions behave as the quasiparticles in materials such as graphene and topological insulators [32,33].

Exactly solvable models are considered indispensable tools to explore the physics of a system and the symmetries behind it. In this paper, we introduce a parity breaking model with an analytical soliton solution. The potential includes powers up to sixth order in the scalar field ϕ, where odd powers of ϕ exist alongside the even, causing a parity asymmetry. In [34], the authors considered a massless Dirac field interacting with a skyrmion-like planar defect in a system that does not respect the parity symmetry. They studied the fermion bound spectrum as well as the scattering of fermions from the localized topological structure and found a closed form for the scattering cross-section for small fermion–skyrmion coupling. Parity or inversion symmetry breaking models with topological solutions are of importance in many areas of physics, for example in the context of superconductivity [35–39], fractional quantum Hall effect [40], mesoscopic electron transport [41], current of abnormal

[a] e-mail: andre.amado@ufpe.br

[b] e-mail: azadeh.mohammadi@df.ufpe.br (corresponding author)

parity [42], heavy-ion collisions [43], nonlinear Schrödinger equations [44] and hydrodynamics [45].

In this paper, we consider a parity-breaking model with two minima where the soliton solutions connect the two vacua in a nonsymmetric form. Unlike the kink of ϕ^4 theory, they have a power-law tail at one side and exponential asymptotics at the other. This behavior can be found most frequently in models where the potential has higher than sextic power in the scalar field [46]. These types of solitons are especially interesting in the context of the soliton–soliton interactions (see, e.g., [47–50]). Although this is not the main focus of this work, we will comment on it when we find it relevant. The goal here is to find the soliton solutions and stability equation analytically as well as to study the interaction of the soliton with boson and fermion fields. We consider two types of interactions with the boson field and Yukawa interaction for the fermion field. The boson bound and scattering states, as well as the fermion zero mode, are expressed in closed analytical forms. However, the massive fermion bound states and energy spectrum are solved numerically. Most analytical results are expressed in terms of the Lambert W function. In Sect. 2, we introduce the model, find the corresponding topological solution and analyze the small oscillations of the soliton. In Sect. 3, we study the interaction of boson and fermion fields with the soliton of our model. Finally, in Sect. 4, we summarize the results of the current work. The appendices provide the details of the calculations.

2 Model

We propose the theory described by the following Lagragian in $1+1$ dimensions

$$\mathcal{L} = \frac{1}{2}\partial_\mu\phi\,\partial^\mu\phi - V(\phi), \tag{1}$$

where the potential term is given by

$$V(\phi) = \frac{\lambda^2}{2}(1-\phi^2)^2(1-\phi)^2. \tag{2}$$

The potential presents two minima, $\phi_0 = \pm 1$, which allows one to obtain solitonic solutions interpolating between them. Although the potential is sixth-order, it has no parity symmetry since odd powers of ϕ are also included, unlike the classical ϕ^6 theory. An equivalent potential could be considered by mapping $\phi \to -\phi$, resulting in an interchange of the roles of the kink and antikink solutions. The coupling λ has mass dimension one, defining a natural mass scale in the system, which we use to rescale all the parameters. Nevertheless, when deemed relevant, we explicit the mass dimension as a function of λ.

Although Lagragian (1) yields a second order equation of motion, thanks to the BPS condition one can obtain an equivalent first order equation

$$\partial_x\phi - (1-\phi^2)(1-\phi) = 0, \tag{3}$$

where the field ϕ is static. Integrating the above equation we find

$$\frac{1}{4}\left[\log\left(\frac{\phi+1}{\phi-1}\right) - \frac{2}{\phi-1}\right] = x + C, \tag{4}$$

where C is the integration constant. We choose the center of the soliton at $\phi(0) = 0$, implying $C = \frac{1}{4}(2 - i\pi)$. This can be solved in terms of Lambert W function.[1] The details of this calculation are provided in Appendix A. The solution is

$$\phi_s(x) = 1 - \frac{2}{1 + W[e^{1+4x}]}. \tag{5}$$

The corresponding antikink solution can be obtained by mapping $\phi \to -\phi$. Figure 1a shows the kink profiles for ϕ^4 and our models. Notice that in the kink profile of our model the parity is explicitly broken. At large x the behavior of the kink is as follows

$$\begin{cases} \phi_s(x) \to -1 + 2e^{1+4x} & x \to -\infty, \\ \phi_s(x) \to 1 - 1/(2x) & x \to \infty. \end{cases} \tag{6}$$

The above asymptotic behavior means that the kink at large x has a long-range power-law fall-off in contrast with the opposite tail, $x \to -\infty$, with exponential asymptotics.

Using the BPS condition, it is straightforward to calculate the energy of the soliton configuration, the so-called classical mass of the soliton,

$$\begin{aligned} M_{cl} &= \int_{-\infty}^{\infty} \mathcal{E}(x)\mathrm{d}x \\ &= \int_{-\infty}^{\infty}\left[\frac{1}{2}\left(\frac{\mathrm{d}\phi}{\mathrm{d}x}\right)^2 + V(x)\right]\mathrm{d}x \\ &= (\lambda)\int_{-1}^{1}(1-\phi^2)(1-\phi)\,\mathrm{d}\phi = \frac{4}{3}\,(\lambda), \end{aligned} \tag{7}$$

where the energy density $\mathcal{E}(x)$ is shown in Fig. 1b for our model and ϕ^4 kink. Interestingly, despite the difference in the energy density of the two models, the resulting mass is the same.

Having the profile of the soliton, it is relevant to analyze the small fluctuations of the boson field described by the linear stability equation

[1] For the properties of Lambert W function check, e.g., [51].

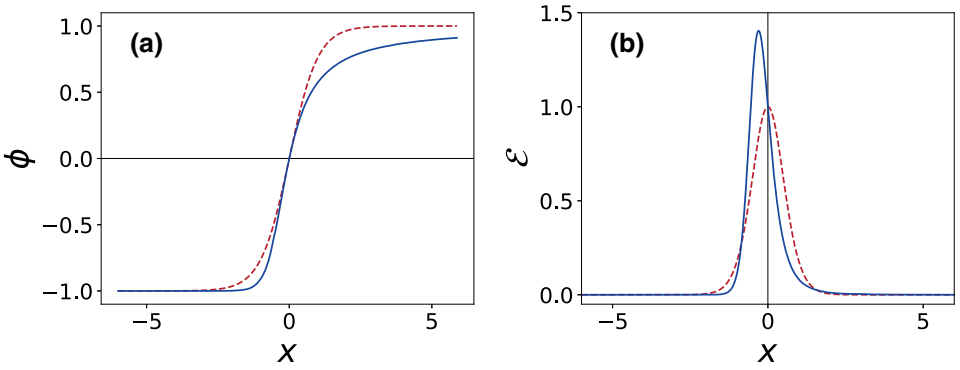

Fig. 1 **a** Soliton profile. **b** Energy density. The solid line (blue) and the dashed line (red) show the soliton in our model and the kink of ϕ^4 theory, respectively

$$\left[-\partial_x^2 + U[\phi(x)]\Big|_{\phi_s(x)}\right]\eta_n(x) = \omega_n^2\eta_n(x)\,, \tag{8}$$

with the stability potential

$$\begin{aligned} U[\phi(x)]\Big|_{\phi_s(x)} &= \frac{d^2V}{d\phi^2}\Big|_{\phi_s(x)} \\ &= \frac{16\left(1 - 8W\left[e^{1+4x}\right] + 6\left(W\left[e^{1+4x}\right]\right)^2\right)}{\left(1 + W\left[e^{1+4x}\right]\right)^4}, \end{aligned} \tag{9}$$

where η_n's are the normal modes of the fluctuations around the static solution. Due to the translational symmetry of the system there exists a zero mode, $\omega_0 = 0$. It is possible to show that it is as follows

$$\eta_0 = \partial_x\phi = \frac{8W\left[e^{1+4x}\right]}{\left(W\left[e^{1+4x}\right] + 1\right)^3}. \tag{10}$$

Now, let us show that the eigenvalues ω_n^2 are non-negative. We can decompose the small fluctuations hamiltonian as

$$H = \left[-\partial_x^2 + U[\phi(x)]\Big|_{\phi_s(x)}\right] \equiv A^\dagger A, \tag{11}$$

where

$$\begin{aligned} A &= -\partial_x + (3\phi_s(x) + 1)\,(\phi_s(x) - 1) \\ &= -\partial_x + \frac{4 - 8W\left[e^{1+4x}\right]}{\left(W\left[e^{1+4x}\right] + 1\right)^2}. \end{aligned} \tag{12}$$

This shows that the above operator H is hermitian and as a result with non-negative eigenvalues [52]. Equivalently, one can multiply both sides of the Eq. (8) by $\eta^\dagger$ from the left and integrate over the whole space which gives

$$\omega^2 = \frac{\int_{-\infty}^{\infty} |A\eta|^2 dx}{\int_{-\infty}^{\infty} |\eta|^2 dx} \tag{13}$$

proving the same, $\omega_n^2 \geq 0$, which makes sense knowing that

$$\frac{d^2V}{d\phi^2}\Big|_{\phi=1} = 0, \quad \frac{d^2V}{d\phi^2}\Big|_{\phi=-1} = 16\,(\lambda^2). \tag{14}$$

Figure 2 shows the stability potential $U(x)$ (panel a) as well as the zero mode η_0 (panel b). As one can see, the potential presents different limits at $x \to \pm\infty$, going to zero at $x \to \infty$. What matters for the bound states is the value of the potential at infinities. When the potential goes to zero from one side (being long-range in this side) makes it impossible to have a gap between the zero mode and the continuum [53]. In contrast, the models with exponentially decaying tails, of which the ϕ^4 kink is an example, have non-zero potential on both sides and therefore a gap. Since the continuum starts at zero and there are no negative ω^2 states, the soliton has no more bound oscillation modes other than the zero mode, which is associated with the translational symmetry.

Knowing that the potential has different limits at $x \to \pm\infty$, only waves whose energy exceeds $U(-\infty)$ are permitted when travelling from the left. In contrast, incoming waves from the right are allowed for lower energies starting from 0, the value of $U(+\infty)$. In this case, oscillations with an energy smaller than $U(-\infty)$ are totally reflected by the potential barrier.

Until now, we have been concerned with the soliton solutions in isolation. In what follows, we consider the interaction of the soliton of our model with other fields, including boson and fermion fields. We analyze two different types of couplings responsible for the soliton–boson interaction, and a Yukawa coupling between the soliton and the Dirac field. In all three cases, we consider the soliton a background field.

3 Interaction with a scalar field

3.1 Model I

First, let us consider the interaction of a real massive scalar field χ with the soliton of our model in the following form

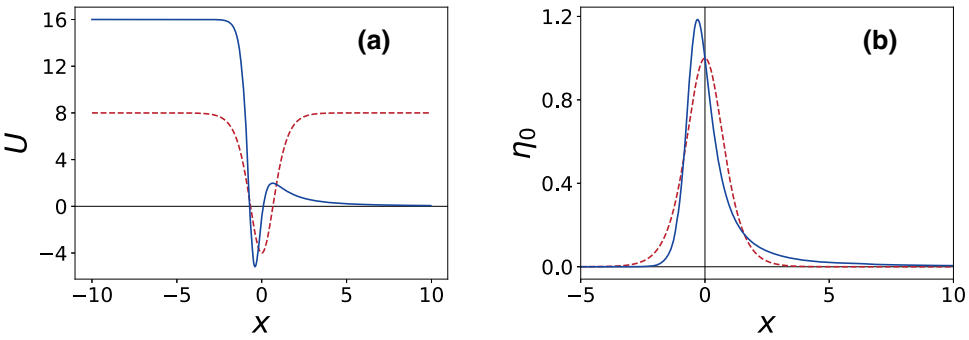

Fig. 2 **a** Stability potential. **b** Zero mode. In both cases, the solid line (blue) and the dashed line (red) show the graphs for our model and the kink of ϕ^4 theory, respectively

$$\mathcal{L} = \frac{1}{2}\partial_\mu\phi\,\partial^\mu\phi - V(\phi) + \frac{1}{2}\partial_\mu\chi\,\partial^\mu\chi + \frac{1}{2}m^2\chi^2 - g\,\phi\,\chi, \tag{15}$$

where m is the mass of the field χ and g is the scalar-soliton coupling constant. This interaction yields a non-homogeneous Klein-Gordon equation

$$(\Box - m^2)\chi = -g\,\phi. \tag{16}$$

Separating the time dependence as $\chi = \chi_s e^{-iEt}$, we find the equation

$$(\partial_x^2 + k^2)\chi_s = g\,\phi, \tag{17}$$

where we define $k^2 \equiv E^2 - m^2$. First consider the bound states, for which we have $k^2 < 0$. The solution to the equation of motion, Eq. (17), is

$$\chi_s(x) = Ae^{\kappa x} + Be^{-\kappa x} + \frac{g}{\kappa}\int^x \sinh\left[\kappa(x-y)\right]\phi\,(y)\;\mathrm{d}y, \tag{18}$$

introducing $k^2 \equiv -\kappa^2$. The first two terms come from the solution of the homogeneous equation and the last one is a particular solution. Focusing only on the integral term in the above solution and performing the change of variables $u = x - y$ results in

$$\begin{aligned} &-\frac{g}{\kappa}\int \sinh(\kappa u)\left(1 - \frac{2}{W\left[e^{1+4(x-u)}\right]+1}\right)\mathrm{d}u \\ &\quad = -\frac{g}{\kappa^2} + \frac{2g}{\kappa}\int \frac{\sinh(\kappa u)}{1+W\left[e^{1+4(x-u)}\right]}\,\mathrm{d}u. \end{aligned} \tag{19}$$

Two more changes of variables, $v = e^{1+4(x-u)}$ followed by $w = W[v]$, allow us to rewrite the integral in a form that can be directly solved

$$\begin{aligned} &-\frac{g}{\kappa^2} - \frac{g}{2\kappa}\int \sinh\left[-\frac{\kappa}{4}\left(\ln(w) + w - 1 - 4x\right)\right]\frac{1}{w}\,\mathrm{d}w \\ &\quad = -\frac{g}{\kappa^2} \\ &\qquad - \frac{g}{4\kappa}\left[\left(-\frac{\kappa}{4}\right)^{-\kappa/4} e^{-\frac{\kappa}{4}(1+4x)}\,\Gamma\left(\frac{\kappa}{4}, -\frac{\kappa}{4}W\left[e^{1+4x}\right]\right)\right. \\ &\qquad \left. - \left(\frac{\kappa}{4}\right)^{\kappa/4} e^{\frac{\kappa}{4}(1+4x)}\,\Gamma\left(-\frac{\kappa}{4}, \frac{\kappa}{4}W\left[e^{1+4x}\right]\right)\right]. \end{aligned} \tag{20}$$

Therefore, the general solution takes the form

$$\begin{aligned} \chi_s(x) = Ae^{\kappa x} + Be^{-\kappa x} &- \frac{g}{\kappa^2} - \frac{g}{4\kappa} \\ &\times \left[\left(-\frac{\kappa}{4}\right)^{-\kappa/4} e^{-\kappa x}\,e^{-\kappa/4}\,\Gamma\left(\frac{\kappa}{4}, -\frac{\kappa}{4}\,W\left[e^{1+4x}\right]\right)\right. \\ &\left. - \left(\frac{\kappa}{4}\right)^{\kappa/4} e^{\kappa x}\,e^{\kappa/4}\,\Gamma\left(-\frac{\kappa}{4}, \frac{\kappa}{4}\,W\left[e^{1+4x}\right]\right)\right]. \end{aligned} \tag{21}$$

To obtain a real χ_s one has to impose the restriction $\kappa = 4n$ where n is an integer number. This means that $E^2 = m^2 - 16n^2$ and also $n < m/4(\lambda)$ following the fact that E^2 is non-negative. Looking at the limit of χ_s when $x \to +\infty$ it is easy to see that, for the solution to be finite, A should be zero. At this limit, the last term in the above expression vanishes and therefore the solution converges to $-g/\kappa^2$. It remains to determine the value of B which can be found by requiring the solution to be finite when $x \to -\infty$. Doing so, it can be shown that

$$B = \frac{g}{16n}\,(-n)^{-n}\;e^{-n}\;\Gamma\,(n)\,. \tag{22}$$

The detailed calculations are provided in Appendix B. Figure 3 shows the bound states for three values of n, 1, 2 and 3. As it can be seen, at the limits $x \to \pm\infty$ the solution converges to $\mp\frac{g}{\kappa^2} = \mp\frac{g}{16n^2}$. This result is expected considering Eq. (17) when $\phi(x \to \pm\infty) = \pm 1$. Notice that, interstingly, bound states are also solitons which means that the original soliton can trap another boson field in the form of a soliton configuration.

Now, let us look at the case $k^2 > 0$ which corresponds to the scattering states. The general solution for this equation is in the form

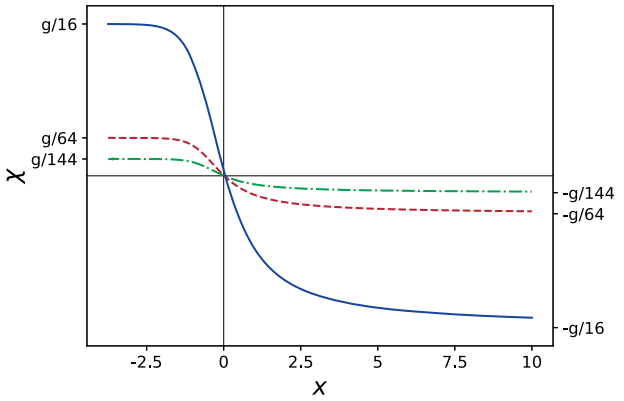

Fig. 3 Bound states for three values $n = 1, 2, 3$

$$\chi_s(x) = Ae^{ikx} + Be^{-ikx} + \frac{g}{k}\int^x \sin[k(x-y)]\,\phi(y)\,\mathrm{d}y, \tag{23}$$

where again the first two terms come from the solution of the homogeneous equation and the last one is a particular solution. Following the same series of change of variables the integral in the above expression changes to

$$-\frac{g}{2k}\int \sin\left[-\frac{k}{4}\left(\ln(w)+w-1-4x\right)\right]\frac{1}{w}\mathrm{d}w = \frac{-ig}{4k}\left[\Gamma(-ik/4, ikw/4)(ik/4)^{ik/4}\,e^{i(1+4x)k/4} - c.c.\right], \tag{24}$$

where $c.c.$ stands for the complex conjugate. After some simplifications, the solution (23) takes the form

$$\chi_s(x) = Ae^{ikx} + Be^{-ikx} + \frac{g}{k^2} + \frac{g}{2k}\,\mathrm{Im} \times\left[\Gamma(-ik/4, ik\,W[e^{1+4x}]/4)\,e^{i[1+4x+\ln(k/4)+i\pi/2]k/4}\right]. \tag{25}$$

To verify the result, one can look at the limits $x \to \pm\infty$. At the limit $x \to +\infty$, the last term in the above solution tends to zero and we recover the expected result using Eq. (17) when $\phi \to 1$

$$\chi_s(x \to +\infty) = Ae^{ikx} + Be^{-ikx} + \frac{g}{k^2}. \tag{26}$$

The same goes for the limit $x \to -\infty$ where the Eq. (25) tends to

$$\chi_s(x \to -\infty) = Ae^{ikx} + Be^{-ikx} - \frac{g}{k^2} + \frac{g}{2k}\,\mathrm{Im} \times\left[\left(\frac{k}{4}\right)^{ik/4} e^{(\pi+i)k/4}\,\Gamma\left(-i\frac{k}{4}\right)e^{ikx}\right]. \tag{27}$$

The last term can be removed through a redefinition of the coefficients A and B, which gives the expected result using Eq. (17) when $\phi \to -1$.

3.2 Model II

Now we introduce a different type of coupling between the soliton field ϕ and the scalar field χ. Consider the following Lagragian

$$\mathcal{L} = \frac{1}{2}\partial_\mu\phi\,\partial^\mu\phi - V(\phi) + \frac{1}{2}\partial_\mu\chi\,\partial^\mu\chi + \frac{1}{2}m^2\chi^2 + g\,\phi\,\chi^2, \tag{28}$$

where the coupling between the fields is analogous to a Yukawa interaction. This interaction yields the equation of motion

$$\left(\Box - m^2\right)\chi - 2g\,\phi\chi = 0. \tag{29}$$

Considering $\chi = \chi_s e^{-iEt}$ and rearranging the terms we arrive at

$$\left(-\partial_x^2 - 2g\,\phi\right)\chi_s = k^2\chi_s. \tag{30}$$

Replacing the solitonic solution of our model in the above equation leads to

$$\left(-\partial_x^2 + \frac{4g}{1+W[e^{1+4x}]}\right)\chi_s = (k^2+2g)\chi_s, \tag{31}$$

which has the formal structure of the Schrödinger equation with energy equal to (k^2+2g). Figure 4 shows the form of the potential term in the above Schrödinger-like equation. In [54], the author solved a similar equation. To map our system to the quantum mechanical system solved in the aforementioned paper, we need first to consider the change of variables $1+4x \to -y$ which results in

$$\left(-\partial_y^2 + \frac{g/4}{1+W[e^{-y}]}\right)\chi_s = \frac{1}{16}(k^2+2g)\chi_s \tag{32}$$

Now, the map between their system and ours is given by $2m/\hbar^2 \to 1$, $V_0 \to g/4$, $E \to (k^2+2g)/16$ and $\sigma \to 1$. As a result, the solution to our system is in the following form

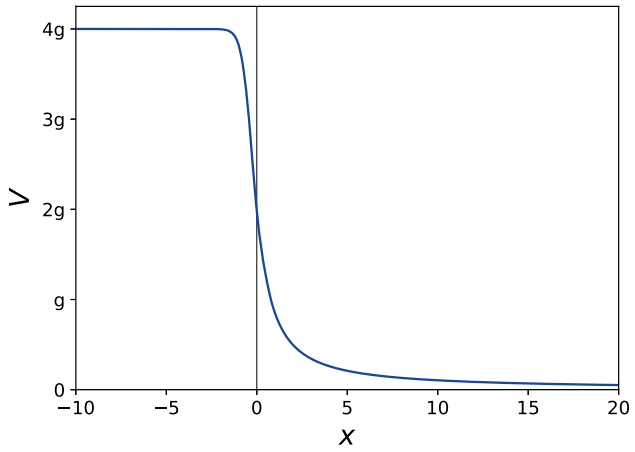

Fig. 4 Potential energy of the Schrödinger-like equation

$$\chi_s = z^{i\delta^-/2} e^{-i\delta^+ z/2} \left(\frac{\mathrm{d}u(z)}{\mathrm{d}z} - i\,\frac{(\delta^+ + \delta^-)}{2}\,u(z) \right) \tag{33}$$

with $z = W\left[e^{1+4x}\right]$, $\delta^\pm = \frac{1}{2}\sqrt{k^2 \pm 2g}$, $a = \left(\delta^+ + \delta^-\right)^2 /(4\delta^+)$,

$$u = C_1\,(i\delta^+ z)^{1-i\delta^-}\,{}_1F_1(1 + i(a - \delta^-); 2 - i\delta^-; i\delta^+ z) + C_2\,U(ia; i\delta^-; i\delta^+ z),$$

where C_1 and C_2 are constants and ${}_1F_1$ and U are the Kummer and Tricomi confluent hypergeometric functions, respectively. The system does not have any bound state, which is easy to recognize from the form of the potential (see Fig. 4). The scattering states from the right and the left are shown in Fig. 5a. Besides that, in the same figure, one can see the scattering from the right where the energy is beneath the threshold required to surpass the barrier. In this case, the wave is totally reflected. Figure 5b shows the reflection coefficient as a function of the momentum for the waves from the right and left. In the case of incoming waves from the right, the reflection coefficient is 1 for momenta associated with energies below the barrier, as expected. Also, for waves coming from both directions, the reflection coefficient drops to zero at high energies since the wave does not see the barrier.

4 Interaction with a fermion field

Fermions can be coupled to the soliton in various ways. We introduce a fermion field ψ coupled to the soliton through a Yukawa coupling in the following form

$$\mathcal{L} = \frac{1}{2}\partial_\mu\phi\,\partial^\mu\phi - V(\phi) + \bar{\psi} i\gamma^\mu\partial_\mu\psi - g\,\phi\,\bar{\psi}\psi, \tag{34}$$

where g is a coupling constant. The resulting equation of motion in the background of the soliton reads

$$i\gamma^\mu\partial_\mu\psi - g\,\phi\,\psi = 0. \tag{35}$$

Opening the spinor field ψ in components as $\psi = e^{-iEt}\begin{pmatrix}\psi_1\\ \psi_2\end{pmatrix}$ one can find the pair of equations

$$\begin{aligned} E\,\psi_1 + \psi_2' - g\,\phi\,\psi_2 &= 0,\\ E\,\psi_2 - \psi_1' - g\,\phi\,\psi_1 &= 0, \end{aligned} \tag{36}$$

where the representation for the Dirac matrices is taken as $\gamma^0 = \sigma_1$, $\gamma^1 = i\sigma_3$ and $\gamma^5 = \sigma_2$. For the case of ϕ^4 model, a zero energy bound state or zero mode is known to exist, which is also the case for our model. The zero mode is given by

$$\psi(x) = \mathcal{N}\begin{pmatrix} e^{-g\int^x \phi(x')\mathrm{d}x'} \\ 0 \end{pmatrix}, \tag{37}$$

where $\mathcal{N}$ is the normalization constant. Since one of the components is null the soliton never receives backreaction from this state and the solution is exact [55]. Performing the above integration we can obtain an explicit solution to the state

$$\psi_1 = \mathcal{N}\exp\left\{-g\int^x \left[1 - \frac{2}{1 + W\left[e^{1+4x'}\right]}\right]\mathrm{d}x'\right\}. \tag{38}$$

Performing the change of variables $y = \exp(1 + 4x)$ this becomes

$$\psi_1 = \mathcal{N}\exp\left\{-g\,x + \frac{g}{2}\int^{e^{1+4x}} \frac{W'[y]}{W[y]}\mathrm{d}y\right\}, \tag{39}$$

using the property of Lambert W function

$$W'[y] = \frac{W[y]}{y\,(1 + W[y])}. \tag{40}$$

Therefore, the wavefunction becomes

$$\psi = \mathcal{N}\begin{pmatrix} \exp\left\{-g\,x + \frac{g}{2}\ln\left[W\left[e^{1+4x}\right]\right]\right\} \\ 0 \end{pmatrix} \tag{41}$$

$$= \mathcal{N}\begin{pmatrix} \left(W\left[e^{1+4x}\right]\right)^{\frac{g}{2}} e^{-g\,x} \\ 0 \end{pmatrix}, \tag{42}$$

with the normalization constant

$$\mathcal{N} = \sqrt{\left(\frac{g}{2}\right)^{g/2}\frac{2\,e^{-g/2}}{\Gamma\,[g/2]}}. \tag{43}$$

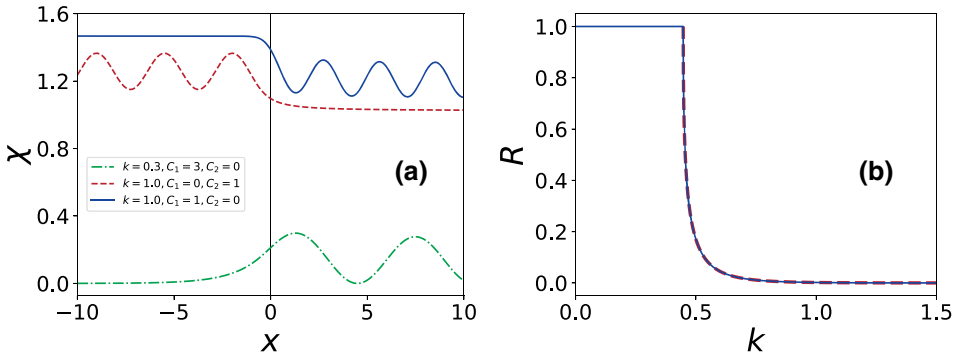

Fig. 5 **a** Boson field continuum states. **b** Reflection coefficient. In both cases, the solid line (blue) and the dashed line (red) show the graphs for scattering from the right and scattering from the left considering $g = 0.1$, respectively. The dot-dashed curve (green) shows the scattering from the right for the case where the energy is below the threshold required to surpass the barrier

Details of the calculation above are supplied in Appendix C. In Fig. 6, we show the fermionic zero mode for two different values of the coupling. The resulting parity asymmetry in the zero mode of our model is visible, especially when the fermion–soliton coupling g increases. Besides that, we solve the equations of motion in (36) for nonzero bound states numerically where the result for the upper and lower components of the first and second fermionic bound states is presented in Fig. 7. A close inspection of the figure reveals that the states do not respect parity. Moreover, we plot the bound and threshold energies as a function of the bound state number as well as the fermion–soliton coupling g in Fig. 8, where the system is solved numerically. It is not difficult to show that the system has energy-reflection symmetry, which is given by γ^1 in our model. In Fig. 8 the symmetry manifests itself by the symmetric form of the spectrum around $E = 0$ line. For very small values of g, the only discrete mode is the zero mode. However, gradually increasing g from zero supports more and more bound states. Besides the bound states, one can explore the scattering ones considering energies above the threshold in the equation of motion (36). We show the upper and lower components of the fermionic scattering states for the scattering from both directions in Fig. 9. Again, it is easy to observe that the states do not respect parity symmetry.

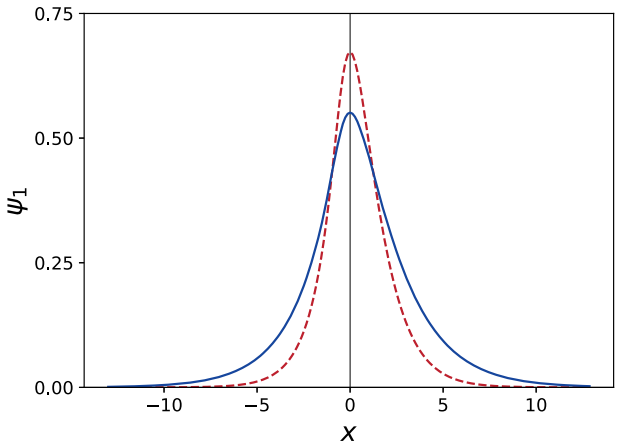

Fig. 6 Fermionic zero mode for $g = 0.5$ (solid curve in blue) and $g = 0.9$ (dashed curve in red)

5 Conclusion

In this work, we have designed a parity-breaking solitonic model where the potential is up to sixth order in the scalar field ϕ, with two minima. The soliton solutions connecting the two minima in a nonsymmetric form, with one long-range power-law tail and one exponential asymptotics, has been solved in terms of the Lambert W function. Although the system lacks Z_2 symmetry, changing $\phi \to -\phi$ only swaps the role of the soliton and antisoliton solutions. We have found the soliton mass, which is equal to the one for the kink of ϕ^4 theory, despite a very different energy density. Studying the linear stability equation for the small perturbations around the static soliton solutions, we have concluded that the only discrete mode is the zero mode associated with the translational invariance, in contrast with the parity-symmetric ϕ^4 model. Besides that, we have studied the interaction of the boson and fermion fields with the soliton considering two different types of interaction terms for the bosonic one and the Yukawa interaction for the fermionic one. The first interaction we have examined has led to a non-homogeneous Klein–Gordon equation with interesting results. For example, we have shown that the boson bound state also acquires the form of a defect, which means that the soliton in our model traps the bosonic field in a kink configuration. Considering the second interaction term, a Yukawa-like interaction, we have shown that one can write the equation of motion in the form of a Schrödinger equation. With a change of variables and mapping the parameters with the results obtained in [54], we have found the bound and continuum states analytically. We have also studied the scattering of the waves from the left and right as well as the reflection coefficient, knowing the barrier shape potential term. We have shown that the reflection coefficient is unity for waves with energies beneath the barrier

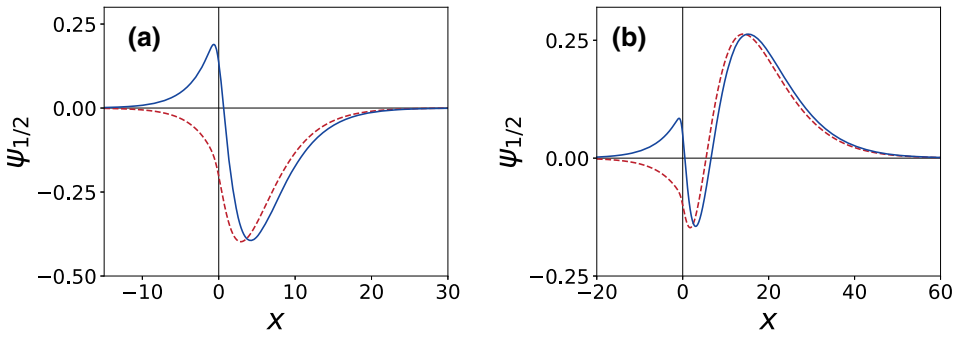

Fig. 7 **a** First fermionic bound state for $g = 0.9$. **b** Second fermionic bound state for $g = 0.9$. The solid (blue) and dashed (red) curves show the upper and lower components, ψ_1 and ψ_2, respectively

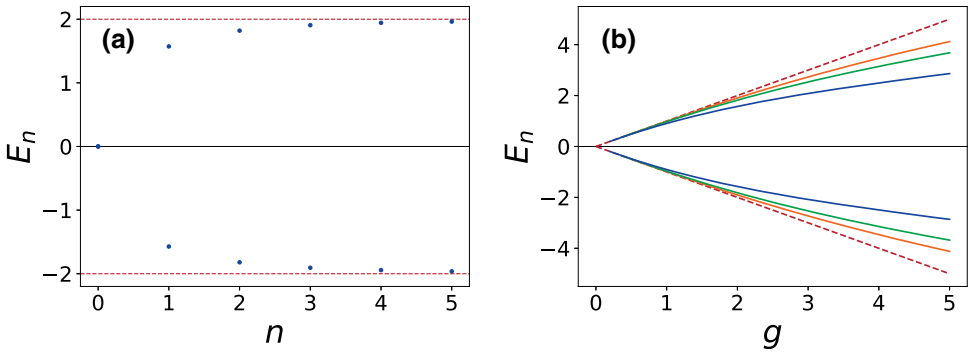

Fig. 8 **a** Fermionic bound energy spectrum for $g = 2$. The dashed lines (red) show the threshold energies. **b** Fermionic bound energy spectrum for the first three bound states as a function of the coupling g. The dashed lines (red) show the threshold energies

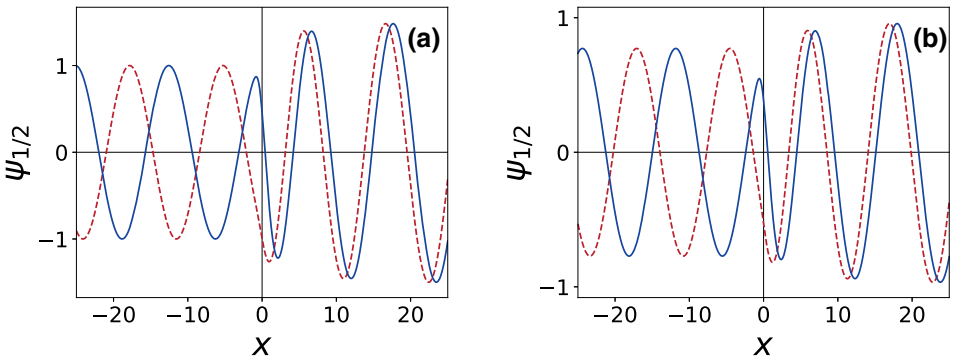

Fig. 9 **a** Fermionic continuum states in the case of the scattering from the right. **b** Fermionic continuum states in the case of the scattering from the left. In both graphs $g = 0.9$ and $k = 0.5$ and also the solid curve (blue) and dashed (red) curve show the upper and lower components, ψ_1 and ψ_2, respectively

and goes to zero at high-energy, as expected. We have solved the system analytically for both types of interactions. It is not common to find systems that can be fully solved analytically, and this makes the model more valuable for follow-up studies and applications. Moreover, in both cases, we have verified that the results match the expectations in the limiting cases where $\phi(x \to \pm\infty) \to \pm 1$. Finally, the interaction of the fermion field with the soliton has been considered. In this case, we have been able to find the normalized fermion zero mode analytically. We have also obtained the nonzero bound energy spectrum as a function of bound state number as well as the fermion–soliton coupling g numerically. The system has energy reflection symmetry given by γ^1 resulting in a symmetric bound energy spectrum. We have shown that, for very small values of the coupling, the only discrete mode is the zero mode, with a growing number of bound states appearing as we gradually increase the coupling. Finally, the scattering oscillating modes for the waves coming from the left and the right have been analyzed.

In future work, we plan to apply the model proposed here to address the soliton–soliton long-range interactions, taking advantage of the analytical properties of the model. Besides that, one can explore how the parity violation affects the charge fractionalization, as first explored in [30].

Acknowledgements AA would like to thank CAPES for financial support under the PNPD fellowship. AM acknowledges the financial support from CNPq (process number 305893/2017-3), CAPES and Universidade Federal de Pernambuco Edital Qualis A. AA and AM are thankful to Carlos Batista for fruitful discussions. Funding was supported by Conselho Nacional de Desenvolvimento Científico e Tecnológico, Coordenação de Aperfeiçoamento de Pessoal de Nível Superior.

Data Availability Statement This manuscript has no associated data or the data will not be deposited. [Authors' comment: It is a theoretical, mostly analytical work, so there is no data.]

Funded by SCOAP[3].

Appendix A: Calculation of the soliton solution

Performing the change of variables $\chi = \phi - 1$ in Eq. 4 we obtain

$$\log\left[\frac{1+2/\chi}{e^{2/\chi}}\right] = 4x - i\pi + 2, \tag{44}$$

which leads to

$$(-1-2/\chi)\, e^{-1-2/\chi} = e^{4x+1}. \tag{45}$$

Recalling that the Lambert W function is defined as the inverse function of

$$f(W) = We^{W}, \tag{46}$$

the previous equation can be written as

$$-1 - 2/\chi = W[e^{4x+1}]. \tag{47}$$

Now solving for χ and reintroducing ϕ we have the final result

$$\phi = 1 - \frac{2}{1 + W\left[e^{4x+1}\right]}. \tag{48}$$

Appendix B: Integration constants of the bound states in model I

We start with the general form of the solution for model I, Eq. (21),

$$\chi_s(x) = Ae^{4nx} + Be^{-4nx} + \frac{g}{16n}\left[f_n(x) - f_{-n}(x) - \frac{1}{n}\right], \tag{49}$$

where

$$f_n(x) \equiv n^n e^{n(1+4x)}\, \Gamma\left(-n, n\, W\left[e^{1+4x}\right]\right). \tag{50}$$

Let us first look at the limit $x \to +\infty$. At this limit, $f_n(x)$ becomes

$$\begin{aligned} f_n(x \to +\infty) &\approx n^n e^{n(1+4x)}\, \Gamma\left(-n, n\left[1 + 4x - \ln(1+4x)\right]\right) \\ &\approx n^n e^{n(1+4x)} \left[\frac{1}{4x} e^{-n(1+4x)} n^{-1-n}\right] = \frac{1}{4nx}. \end{aligned} \tag{51}$$

Therefore,

$$\lim_{x\to+\infty} f_n(x) = 0, \tag{52}$$

and similarly

$$\lim_{x\to+\infty} f_{-n}(x) = 0. \tag{53}$$

Since the A term diverges in this limit and there is no other term to compensate it, the constant A should be set to zero.

Now considering the limit $x \to -\infty$ we can determine the remaining constant B. Using the expansion of the Lambert function for small arguments we have

$$\begin{aligned} f_n(x \to -\infty) &\approx n^n e^{n(1+4x)}\, \Gamma\left(-n, n\, e^{1+4x}\right) \\ &\approx n^n e^{n(1+4x)}\, \frac{1}{n!} \\ &\quad \times \left[\frac{e^{n\, e^{1+4x}}}{\left(n\, e^{1+4x}\right)^n}(n-1)! + (-1)^n \Gamma\left(0, n\, e^{1+4x}\right)\right] \\ &\approx n^n e^{n(1+4x)} \\ &\quad \times \left\{\frac{e^{n\, e^{1+4x}}}{n\left(n\, e^{1+4x}\right)^n} + \frac{(-1)^n}{n!}\left[-\gamma - \ln\left(n\, e^{1+4x}\right) + n\, e^{1+4x}\right]\right\}. \end{aligned}$$

In the limit $x \to -\infty$, we can ignore the second term and replace $e^{n\, e^{1+4x}}$ with 1, which gives

$$\lim_{x\to-\infty} f_n(x) = \frac{1}{n}. \tag{54}$$

We need to deal with $f_{-n}(x)$ differently. For this function, we have

$$\begin{aligned} f_{-n}(x \to -\infty) &\approx (-n)^{-n} e^{-n(1+4x)}\, \Gamma\left(n, -n\, e^{1+4x}\right) \\ &= (-n)^{-n} e^{-n(1+4x)} \left[\Gamma(n) - \gamma\left(n, -n\, e^{1+4x}\right)\right], \end{aligned} \tag{55}$$

where $\gamma(s,z)$ is the lower incomplete gamma function. Therefore, we obtain

$$f_{-n}(x\to-\infty) \approx (-n)^{-n}e^{-n(1+4x)}\left[\Gamma(n)-\frac{\left(-n\,e^{1+4x}\right)^n}{n}\right] \quad (56)$$

$$= (-n)^{-n}e^{-n}\,\Gamma(n)\,e^{-4nx}-\frac{1}{n}. \quad (57)$$

The first term diverges at $x\to-\infty$ and should be cancelled by the B term in the full solution. As a result, Eq. (49) becomes

$$\chi_s(x)=\frac{g}{16n} \times\left[f_n(x)-f_{-n}(x)-\frac{1}{n}-(-n)^{-n}e^{-n}\,\Gamma(n)\,e^{-4nx}\right]. \quad (58)$$

Appendix C: Normalization of the fermionic zero mode

In Eq. (41), we can find the normalization factor in the following way

$$\mathcal{N}^2 = 1\Big/\int_{-\infty}^{\infty}\psi_1^*\psi_1\,\mathrm{d}x = 1\Big/\int_{-\infty}^{\infty}e^{-2g\,x}\left(W\left[e^{1+4x}\right]\right)^g\,dx\ . \quad (59)$$

Choosing the transformation $y=e^{1+4x}$, it results in

$$\mathcal{N}^2 = 1\Big/\int_0^{\infty}\frac{e^{-\frac{g}{2}[\ln(y)-1]}}{4\,y}\,(W[y])^g\,dy \quad (60)$$

$$= e^{-g/2}\Big/\int_0^{\infty}\frac{1}{4\,y^{1+g/2}}\,(W[y])^g\,dy\ . \quad (61)$$

Now let's consider the change of variables $w=W(y)$ (notice that $y=we^w$, by the very definition of the Lambert W function). Therefore,

$$\mathcal{N}^2 = 4e^{-g/2}\Big/\int_0^{\infty}\frac{w^g}{(we^w)^{1+g/2}}\,(1+w)\,e^w\,dw\ , \quad (62)$$

which leads to

$$\mathcal{N}^2=\left(\frac{g}{2}\right)^{g/2}\frac{2\,e^{-g/2}}{\Gamma[g/2]}\,. \quad (63)$$

References

1. Y.M. Shnir, *Topological and Non-topological Solitons in Scalar Field Theories* (Cambridge University Press, Cambridge, 2018)
2. F. Abdullaev, S. Darmanyan, P. Khabibullaev, J. Engelbrecht, *Optical Solitons* (Springer Publishing Company, Incorporated, New York, 2014)
3. T. Vachaspati, *Kinks and Domain Walls: An Introduction to Classical and Quantum Solitons* (Cambridge University Press, Cambridge, 2006)
4. Y.S. Kivshar, G. Agrawal, *Optical Solitons: From Fibers to Photonic Crystals* (Academic Press, New York, 2003)
5. R. Rajaraman, *Solitons and Instantons* (North Holland, Amsterdam, 1982)
6. A. Fert, N. Reyren, V. Cros, Magnetic skyrmions: advances in physics and potential applications. Nat. Rev. Mater. **2**(7), 17031 (2017)
7. S.S.P. Parkin, M. Hayashi, L. Thomas, Magnetic domain-wall racetrack memory. Science **320**(5873), 190–194 (2008)
8. T. Koyama, D. Chiba, K. Ueda, K. Kondou, H. Tanigawa, S. Fukami, T. Suzuki, N. Ohshima, N. Ishiwata, Y. Nakatani et al., Observation of the intrinsic pinning of a magnetic domain wall in a ferromagnetic nanowire. Nat. Mater. **10**(3), 194 (2011)
9. A.L. Fetter, P.C. Hohenberg, Theory of type II superconductors, in *Superconductivity*, ed. by J. Ruban (Routledge, London, 2018), pp. 817–923
10. D. Kleckner, W.T.M. Irvine, Creation and dynamics of knotted vortices. Nat. Phys. **9**(4), 253 (2013)
11. O.M. Auslaender, L. Luan, E.W.J. Straver, J.E. Hoffman, N.C. Koshnick, E. Zeldov, D.A. Bonn, R. Liang, W.N. Hardy, K.A. Moler, Mechanics of individual isolated vortices in a cuprate superconductor. Nat. Phys. **5**(1), 35 (2009)
12. A.A. Abrikosov, Nobel lecture: type-II superconductors and the vortex lattice. Rev. Mod. Phys. **76**(3), 975 (2004)
13. M.V. Polyakov, H.-D. Son, Nucleon gravitational form factors from instantons: forces between quark and gluon subsystems. J. High Energy Phys. **2018**(9), 156 (2018)
14. C. Schneider, G. Torgrimsson, R. Schützhold, Discrete worldline instantons. Phys. Rev. D **98**(8), 085009 (2018)
15. C. Csáki, Y. Shirman, J. Terning, M. Waterbury, Kaluza-klein monopoles and their zero modes. Phys. Rev. Lett. **120**(7), 071603 (2018)
16. D.F. Jackson Kimball, D. Budker, J. Eby, M. Pospelov, S. Pustelny, T. Scholtes, Y.V. Stadnik, A. Weis, A. Wickenbrock, Searching for axion stars and q-balls with a terrestrial magnetometer network. Phys. Rev. D **97**(4), 043002 (2018)
17. M. Hindmarsh, K. Rummukainen, D.J. Weir, New solutions for non-abelian cosmic strings. Phys. Rev. Lett. **117**(25), 251601 (2016)
18. T. Schaefer, Instanton effects in qcd at high baryon density. Phys. Rev. D **65**(9), 094033 (2002)
19. A. Vilenkin, E.P.S. Shellard, *Cosmic Strings and Other Topological Defects* (Cambridge University Press, Cambridge, 2000)
20. A. Kusenko, M. Shaposhnikov, Supersymmetric q-balls as dark matter. Phys. Lett. B **418**(1–2), 46–54 (1998)
21. G. t Hooft, Magnetic monopoles in unified theories. Nucl. Phys. B **79**(CERN–TH–1876), 276–284 (1974)
22. M. Alcon-Camas, A.E. El-Taher, H. Wang, P. Harper, V. Karalekas, J.A. Harrison, J.-D. Ania-Castañón, Long-distance soliton transmission through ultralong fiber lasers. Opt. Lett. **34**(20), 3104–3106 (2009)
23. P. Marin-Palomo, J.N. Kemal, M. Karpov, A. Kordts, J. Pfeifle, M.H.P. Pfeiffer, P. Trocha, S. Wolf, V. Brasch, M.H. Anderson et al., Microresonator-based solitons for massively parallel coherent optical communications. Nature **546**(7657), 274 (2017)
24. H.A. Haus, W.S. Wong, Solitons in optical communications. Rev. Mod. Phys. **68**(2), 423 (1996)
25. A. Mohammadi, E.R.B. de Mello, Finite temperature bosonic charge and current densities in compactified cosmic string spacetime. Phys. Rev. D **93**(12), 123521 (2016)

26. S.S. Gousheh, A. Mohammadi, L. Shahkarami, Casimir energy for a coupled fermion-kink system and its stability. Phys. Rev. D **87**(4), 045017 (2013)
27. G.W. Semenoff, P. Sodano, Stretching the electron as far as it will go. arXiv preprint (2006). arxiv:cond-mat/0605147
28. S. Burger, K. Bongs, S. Dettmer, W. Ertmer, K. Sengstock, A. Sanpera, G.V. Shlyapnikov, M. Lewenstein, Dark solitons in Bose–Einstein condensates. Phys. Rev. Lett. **83**(25), 5198 (1999)
29. A. Melfo, N. Pantoja, J.D. Tempo, Fermion localization on thick branes. Phys. Rev. D **73**(4), 044033 (2006)
30. R. Jackiw, C. Rebbi, Solitons with fermion number 1/2. Phys. Rev. D **13**(12), 3398 (1976)
31. W.P. Su, J.R. Schrieffer, A.J. Heeger, Solitons in polyacetylene. Phys. Rev. Lett. **42**(25), 1698 (1979)
32. A.H. Castro Neto, F. Guinea, N.M.R. Peres, K.S. Novoselov, A.K. Geim, The electronic properties of graphene. Rev. Mod. Phys. **81**(1), 109 (2009)
33. X.-L. Qi, S.-C. Zhang, Topological insulators and superconductors. Rev. Mod. Phys. **83**(4), 1057 (2011)
34. D. Bazeia, A. Mohammadi, Dirac field in the background of a planar defect. Phys. Lett. B **779**, 420–424 (2018)
35. H. Watanabe, Y. Yanase, Group-theoretical classification of multipole order: emergent responses and candidate materials. Phys. Rev. B **98**(24), 245129 (2018)
36. J. Ishizuka, Y. Yanase, Odd-parity multipole fluctuation and unconventional superconductivity in locally noncentrosymmetric crystal. Phys. Rev. B **98**(22), 224510 (2018)
37. J. Ruhman, V. Kozii, F. Liang, Odd-parity superconductivity near an inversion breaking quantum critical point in one dimension. Phys. Rev. Lett. **118**(22), 227001 (2017)
38. Y. Wang, G.Y. Cho, T.L. Hughes, E. Fradkin, Topological superconducting phases from inversion symmetry breaking order in spin-orbit-coupled systems. Phys. Rev. B **93**(13), 134512 (2016)
39. P.B. Wiegmann, Parity violation and superconductivity in two-dimensional correlated electronic systems. Phys. Rev. Lett. **65**(16), 2070 (1990)
40. N. Read, D. Green, Paired states of fermions in two dimensions with breaking of parity and time-reversal symmetries and the fractional quantum hall effect. Phys. Rev. B **61**(15), 10267 (2000)
41. P.S. Deo, How general is Legett's conjecture for a mesoscopic ring?. arXiv preprint. (1995). arXiv:cond-mat/9505125
42. E. Fradkin, E. Dagotto, D. Boyanovsky, Physical realization of the parity anomaly in condensed matter physics. Phys. Rev. Lett. **57**(23), 2967 (1986)
43. B.I. Abelev, M.M. Aggarwal, Z. Ahammed, A.V. Alakhverdyants, B.D. Anderson, D. Arkhipkin, G.S. Averichev, J. Balewski, O. Barannikova, L.S. Barnby et al., Azimuthal charged-particle correlations and possible local strong parity violation. Phys. Rev. Lett. **103**(25), 251601 (2009)
44. J. Yang, S. Nixon, Stability of soliton families in nonlinear Schrödinger equations with non-parity-time-symmetric complex potentials. Phys. Lett. A **380**(45), 3803–3809 (2016)
45. A. Lucas, P. Surówka, Phenomenology of nonrelativistic parity-violating hydrodynamics in 2+ 1 dimensions. Phys. Rev. E **90**(6), 063005 (2014)
46. M.A. Lohe, Soliton structures in p (φ) 2. Phys. Rev. D **20**(12), 3120 (1979)
47. N.S. Manton, Forces between kinks and antikinks with long-range tails. J. Phys. A Math. Theor. **52**(6), 065401 (2019)
48. I.C. Christov, R.J. Decker, A. Demirkaya, V.A. Gani, P.G. Kevrekidis, R.V. Radomskiy, Long-range interactions of kinks. Phys. Rev. D **99**(1), 016010 (2019)
49. I.C. Christov, R.J. Decker, A. Demirkaya, V.A. Gani, P.G. Kevrekidis, A. Khare, A. Saxena, Kink–kink and kink–antikink interactions with long-range tails. Phys. Rev. Lett. **122**(17), 171601 (2019)
50. E. Belendryasova, V.A. Gani, Scattering of the $\varphi 8$ kinks with power-law asymptotics. Commun. Nonlinear Sci. Numer. Simul. **67**, 414–426 (2019)
51. R.M. Corless, G.H. Gonnet, D.E.G. Hare, D.J. Jeffrey, D.E. Knuth, On the Lambert W function. Adv. Comput. Math. **5**(1), 329–359 (1996)
52. D. Bazeia, M.M. Santos, Classical stability of solitons in systems of coupled scalar fields. Phys. Lett. A **217**(1), 28 (1996)
53. A. Khare, A. Saxena, Family of potentials with power law kink tails. J. Phys. A Math. Theor. **52**(36), 365401 (2019)
54. A.M. Ishkhanyan, The Lambert-w step-potential—an exactly solvable confluent hypergeometric potential. Phys. Lett. A **380**(5–6), 640–644 (2016)
55. A. Amado, A. Mohammadi, Coupled fermion-kink system in Jackiw–Rebbi model. Eur. Phys. J. C **77**(7), 465 (2017)